

GIOVE-A PRECISE ORBIT DETERMINATION FROM MICROWAVE AND SATELLITE LASER RANGING DATA - FIRST PERSPECTIVES FOR THE GALILEO CONSTELLATION AND ITS SCIENTIFIC USE

E. Schönemann⁽¹⁾, T. A. Springer⁽²⁾, M. Otten⁽²⁾, M. Becker⁽¹⁾, J. Dow⁽²⁾

(1) *Institut für Physikalische Geodäsie, Technische Universität Darmstadt, Petersenstraße 13, 64287 Darmstadt, Germany, +49(6151)164511, Schoenemann@ipg.tu-darmstadt.de, Becker@ipg.tu-darmstadt.de*

(2) *Navigation Support Office, European Space Operations Centre, Robert Bosch Straße 5, 64293 Darmstadt, Germany, +49(6151) 902029, Tim.Springer@esa.int, Michiel.Otten@esa.int, John.Dow@esa.int*

1 Introduction

The navigation office of the European Space Operations Centre (ESOC) is engaged in various activities using the GIOVE-A observations, recorded at the GALILEO Experimental Sensor Stations (GESS). Main topics are testing and improvement of the NAPEOS software installed at ESOC. The overall goal is the scientific use of the future GALILEO constellation within the tasks and goals of ESA and the International GNSS Service (IGS). Key elements of the future applications are proper modelling of GALILEO orbits and assessment of quality and performance of the GALILEO observables.

Since the first definition of GALILEO signals a wide range of theoretical analyses have been published evaluating the signal quality and compare their performance to the GPS signals. Several publications, as [8] and [10] show the expected advantages of the new frequencies and code modulation schemata.

Since the start of GIOVE-A on December 28th 2005 different tests were carried out analysing the quality of the new code and phase observables, as in [12] and [2]. All these tests demonstrate the advantages of the new signal structure. In general the reduction of the noise by factor of 4-5 [12] as well as a reduction of the code multipath by approximately a factor of 1.2 (GPS C1C versus GIOVE-A C1B/C1C) could be seen.

As the comparison of observations is done indirectly (GPS and GIOVE-A have different orbits) and the data basis used for most analyses published up to now is sparse, a deeper analysis of the signal quality parameters seemed appropriate. These analyses, presented in part one of this paper, are based on a broad base of data from most of the GESS. Because of the difficulty to access the phase multipath directly we first evaluated the signal strength and the code multipath, which gave a first hint of the multipath behaviour. In order to compare GPS and GIOVE-A data directly only data received from equal elevations and azimuths was used. Following we present an analysis of the phase residual, derived by precise point positioning.

The second part of this paper focuses on the precise orbit determination of the GIOVE-A spacecraft. The NAPEOS software used at the ESOC Navigation Support Office allows the combined or alternative use of both microwave and satellite laser ranging observations. The two methods are different due to different tracking networks and the different sensitivity of the observables to atmospheric effects and in their noise level. We will present the orbit results focusing on internal orbit consistency checks and SLR validation of the microwave based orbits. Furthermore, a detailed look at the solar radiation pressure parameters is presented.

Station name	Location	Country	Data
GIEN	Turin	Italy	used
GKIR	Kiruna	Sweden	used
GKOU	Kourou	French Guyana	used
GLPG	La Plata	Argentina	used
GMAL	Malindi	Kenya	not used
GMIZ	Mizusawa	Japan	used
GNNO	New Norcia	Australia	used
GNOR	Noordwijk	Netherlands	used
GOUS	Dunedin	New Zealand	used
GTHT	Tahiti	French Polynesia	used
GUSN	Washington	USA	used
GVES	Vesleskarvet	Antarctica	not used
GWUH	Wuhan	China	not used

Tab. 1: GESS stations used for analyses

2 Data analysis

2.1 Microwave analysis

For the GIOVE-A signal analysis and precise orbit determination we use the RINEX data of all GESS stations available from the GIOVE archiving facility. All stations are equipped with GPS/GALILEO antennas, built by “Space Engineering S.p.A.” and GALILEO Experimental Test Receiver (GETR), built by Septentrio. The data, containing tracking data of all GPS satellites and the GIOVE-A satellite, is given in the RINEX 3.00 data format with a sampling of 1 second. To save on storage space, for the long term analyses, e.g. orbit determination, the RINEX data is decimated to 30 seconds sampling and Hatanaka compressed, using a test version of the Hatanaka software for the RINEX 3.00 format [7].

The signal analyses shown in the first part of this paper were carried out using GNU Octave, an open source program for performing numerical computations and different scripts developed by the “Institut für Physikalische Geodäsie, Technische Universität Darmstadt” (IPGD). These analyses cover a selection of the designated GALILEO signals recorded on the GESS (Tab. 1) within a time span from December 16th until 27th, 2006. Within this time period the current GPS signals, as well as the GALILEO signals E1 and E5, shown in Tab. 2 were recorded. The table shows furthermore the applied code modulation schemata [5], as well as the RINEX observation type specifications [6] which we will use henceforth.

The stations used within this analyses show a quite similar performance in general. There are stations with different behaviour for single signals, as for example GIEN with a stronger code multipath behaviour on C1B and C1A, but no station with considerably different performance could be identified. The averaging over the data from all sites reduces the station dependent effects like multipath and atmosphere to a large extent and gives a good indication of the mean signal performance.

The analysed phase residuals were taken from the processing of part two of this paper. Hence they include observation data of 150 days and were limited to the GIOVE-A C1C/L1C and C7Q/L7Q signals.

We have analysed the data in the time period of 12-December-2006 (doy 346) until 26-May-2007 (doy 146). In this period there is a period where no GIOVE-A data was available due to maintenance of the spacecraft. This gap was from 12-28 February 2007. So in total we have analysed 150 days of microwave data.

Signal	Components	RINEX Name	Modulation Type	Carrier	RINEX Name
E5	E5a-I data	C5I	BPSK(10)	1176.45MHz	L5I
	E5a-Q pilot	C5Q			L5Q
	E5b-Q pilot	C7Q	AltBOC(15,10)	1207.14MHz	L7Q
	E5a+E5b	C8Q			L8Q
E1	E1-A	C1A	BOC(15,2.5)	1575.42MHz	L1A
	E1-B data	C1B	BOC(1,1)		L1B
	E1-C pilot	C1C			L1C
G1	C/A data	C1C	BPSK(1)	1575.42MHz	L1C
	P data	C1P	BPSK		L1P
G2	P data	C2P	BPSK	1227.60MHz	L2P

Tab. 2: GIOVE-A signals used in this study

Because there are some differences between the results before and after this gap in February many of the statistics are given for the first and second part separately. The first part covers 12-December-2006 until 11-February-2007. The second part covers 1-March-2007 until 26-May-2007.

The precise orbit determination is performed using the NAPEOS software. NAPEOS, standing for Navigation Package for Earth Observation Satellites, is a general purpose software package for orbit determination, prediction and control, supporting all phases of an Earth Observation Mission in terms of mission preparation and operations. NAPEOS has been designed to support ESA Earth Observation missions, but there are other types of Earth orbiter missions of interest to ESA and other agencies, for which NAPEOS could provide support (in part or whole). The orbit modelling part of NAPEOS is designed to handle any type of Earth orbiter and the orbit determination part is designed to process the full range of current measurement types, including different types of ground-based range and DOPPLER measurements, angular measurements, height measurements from a radar altimeter, and inter-satellite ranges and range-rates.

For the GIOVE-A analysis the three main NAPEOS programmes used are GnssObs, Bahn, and Multiarc. GnssObs reads, cleans, and decimates the RINEX data and converts the data into the NAPEOS internal tracking data format. The data cleaning is mainly based on screening the well known Melbourne-Wuebbena combination, but also the ionosphere combination (L1 - L2) and the difference between the ionosphere free code and phase measurements (PC - LC) are examined. In addition to this the receiver clocks are computed. This computation provides an additional data check possibility and it ensures that the receiver clocks are properly initialized for the main parameter estimation step. Furthermore, the phase

observations are aligned to the code observations thus initializing the carrier phase ambiguities. In this alignment care is taken to retain the integer character of the phase ambiguities by adjusting only in steps of full phase cycles. The NAPEOS tracking data format will contain the ionosphere free linear combination, for both code and phase, of the RINEX observations. For GPS the ionosphere free linear combination is based on the combination of C1P and C2P code and L1P and L2P phase measurements. GIOVE-A offers several different observations allowing for many different ionosphere free observations. For most of the work presented in this paper we have used the ionosphere free linear combination of the C1C and C7Q and L1C and L7Q observations for code and phase respectively.

The next step, Bahn, performs the parameter estimation. In this step we use the ionosphere free code and phase observations at a sampling rate of 5 minutes, and we have applied an cut-off elevation angle of 5 degrees. To account for the fact that the data noise increases with decreasing elevation we apply an elevation dependent weighting scheme. For this we have assumed that the data noise is proportional to the function $1/\cos(z)$ where z is the zenith angle. The data is processed in batches of 24 hours, thus resulting in 1-day arc solutions. In the process the orbits and clocks of the GPS satellites are fixed to the values as provided by the IGS based on the so-called IGS final orbits and clocks [4]. The estimated parameters in these daily solutions are the GIOVE-A state vector, 5 dynamical orbit parameters (D0, Y0, B0, BC, BS) from the extended CODE orbit model [1] and [14], GIOVE-A clock offset for each epoch, all receiver clock offsets for each epoch, one GPS-GIOVE-A “intersystem bias” per day for each stations except a selected reference station, the carrier phase ambiguities (non-integer resolved). The station coordinates are estimated but tightly constrained (1mm) to their a priori value. The a priori station coordinates were obtained by combining the full set of daily solutions. The troposphere effects are modelled by computing the troposphere zenith delay with the Saastamoinen function [11] with temperature and pressure from the standard atmosphere model. This zenith delay is mapped to the required elevation using the Niell Dry Mapping Function (NMF) [9]. The remaining troposphere disturbances are estimated using 2 hourly piece wise linear tropospheric zenith delays. These zenith delays are mapped to the required elevation using the Niell Wet mapping function.

Despite the fact that the 13 GESS stations do provide a very good global coverage it is expected that 24 hour solutions will not give the most precise GIOVE-A orbit estimates. To generate longer arc solutions we will use the Multiarc program. This is a tool which has recently been added to the NAPEOS software package. It allows a rigorous combination of normal equations, also referred to as normal equation stacking, which are generated by Bahn. During the normal equation combination also the satellite orbit parameters may be rigorously combined thus effectively leading to multi day orbital arcs. For the work presented in this paper we have used Multiarc to generate solutions with arc lengths of 1-, 2-, 3-, 4-, and 5-days. Multiarc was also used to compute accurate a priori station coordinates by stacking all available 1-day normal equations.

2.2 Satellite Laser Ranging (SLR) analysis

Beside the 13 GESS stations GIOVE-A is also tracked by more then 17 different SLR stations over the world. For most periods of the mission the tracking has been consistent enough to allow for Precision Orbit Determination (POD) of GIOVE-A using only the SLR data. As the SLR data is completely independent of the microwave data the resulting orbit solutions will be to a large extend independent as well and thus can be used to give an indication of the achieved precision of the different microwave solutions.

The orbit determination strategy used for the SLR solutions is very similar to the one used for the microwave orbits with the main difference being the increased arc-length of 7 days. The same satellite parameters are estimated as with the microwave solutions: the GIOVE-A state vector and 5 dynamical orbit parameters (D0, Y0, B0, BC, BS) from the extended CODE orbit model. No further parameters need to be estimated and all corrections applied to the SLR data are according to the IERS-2003 standards and for stations coordinates the rescaled ITRF-2005 solution is used. As the noise level of the SLR data is very low the measurement can also be directly used to give an indication of the radial precision of the different microwave solutions by computing the SLR residuals without using them in the estimation process itself.

2.3 Combined microwave and SLR analysis

In this step the SLR data was added to the microwave data in the 24-hour solutions. For the weighting we used 100 mm for SLR and 1000 mm and 10 mm for GIOVE-A and GPS code and phase observables. The only change in the analysis strategy in this case was that the SLR data was now processed in 24-hour solutions and not in 7-day batches. All the processing options remained as described in the two previous sections. The resulting 1-day solutions, or rather normal equations, were used in Multiarc to generate combined solutions of different arc lengths.

3 Observation data quality

3.1 Code

Signal to noise ratio

The signal to noise ratio SNR is strongly dependent on the transmitter (satellite), the signal path (atmosphere) and the receiver (ground station, antenna, receiver, cable, etc.). Hence the SNR can not be seen as an absolute value. The SNR is special for the position, the equipment and the time. Furthermore the derivation of the SNR depends on the receiver and the firmware used. Out of that SNR from different receivers is not comparable in an easy way. Nevertheless, using only one type of receiver, assuming similar effects on all the different signals at the same epoch and taking averages over a longer time span, the relationship between the signals is expected to be constant. Based on this assumption we can use the SNR values given in the GESS-RINEX files straight away.

In order to compare the GPS with the GIOVE-A SNR the corresponding SNR values of all stations and all days were ordered by satellite position into a grid with a width of 5 degree in azimuth and elevation. For the evaluation we took the cells filled in for both GPS and GIOVE-A and computed the median over all the cells of equal elevation. The median per elevation for each signal is shown in Fig. 1.

As can be seen from the figure the signal strength of the GIOVE-A C8Q ranks best, followed by the GPS C1C, GIOVE-A C7Q, C5I/C5Q, C1A, C1B/C1C. The weakest signal is found for the GPS C1P/C2P, with a maximum signal strength of 40 (receiver dependent unit, approximately dB) in zenith. Comparing the open signals GPS versus GIOVE-A, GPS C1C is considerably stronger than the GIOVE-A C1B/C1C. According to the specification of the interface control documents of GPS and GALILEO, GIOVE-A C1B/C1A should show up with a stronger signal strength than GPS C1C. The power levels guaranteed on the earth surface are -160 dBW for GPS [3] and -158 dBW for the future GALILEO satellite signals excepted the BOC(10,5) and BOC(n,m) modelled signals, for which a power level of even -155dBW [5] is guaranteed. But looking on the signal to noise ratios shown in Fig. 1, it shows, that the GIOVE-A C1B/C1C is worse by approximately 4dB than the GPS C1C. An increasing of the signal power for the future GALILEO satellites should even increase the signal performance, shown within this paper.

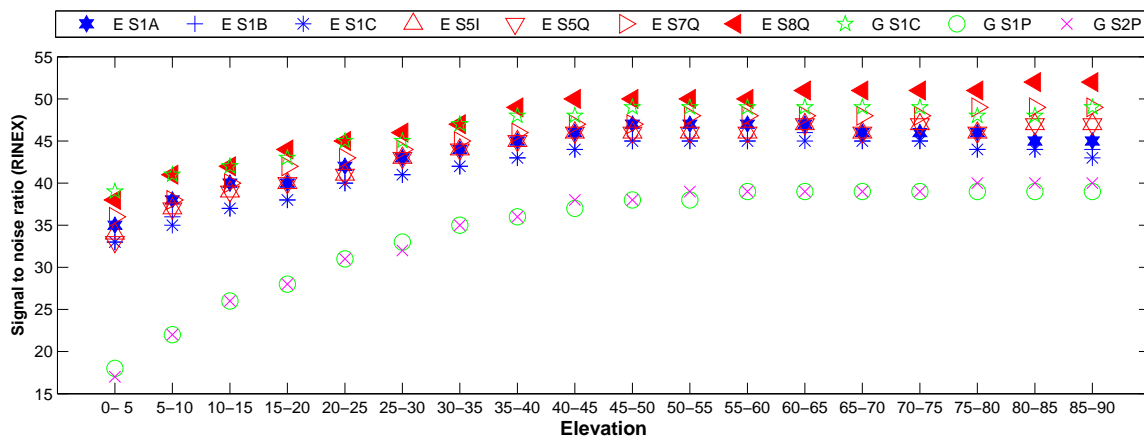


Fig. 1: Signal to noise ratio, GPS versus GIOVE - A

Code tracking noise

For signals containing data and pilot components, as in the case of GIOVE-A, the code tracking noise can easily be computed as the difference between the data and the pilot signal. The advantage of this computation schema is that both signals are influenced by identical error sources (atmospheric errors, multipath errors, receiver errors, etc.). Based on the assumption of equal uncertainties in the two components the resulting noise values were divided by the square root of two to specify the noise level of each part according to the laws of error propagation. Tab. 3 shows the code tracking noise for the two analysed GIOVE-A codes sorted by elevation. The median code tracking noise, 0.62 m for C1B/C1C and 0.35m for C5I/C5Q, for observations below an elevation of 5°. For the C1B and C1C codes the noise median stays below 0.2 m

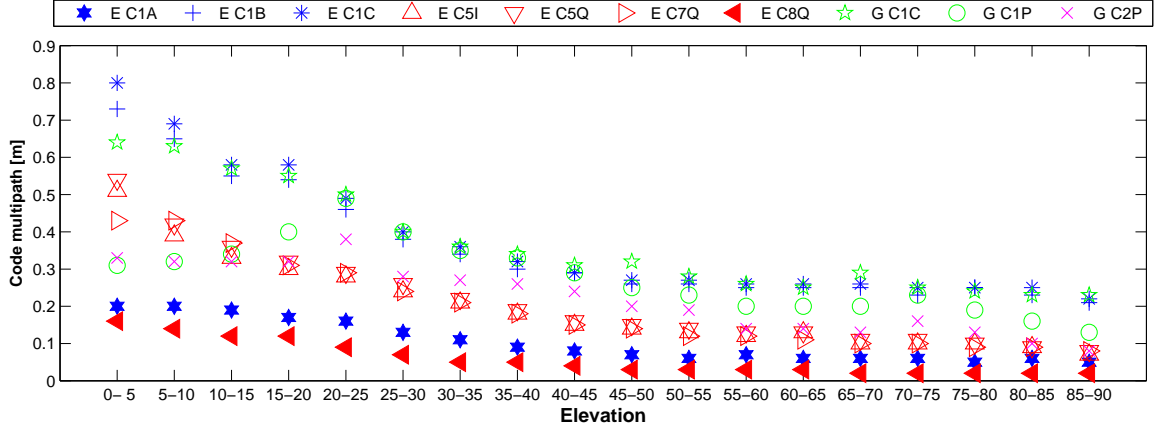


Fig. 2: Code multipath, GPS versus GIOVE - A

for an elevation above 25° , whereas the median for the codes C5I and C5Q for elevations above 35° even comes down below 0.1 m. The results discussed above confirm the code tracking noise values published previously as e.g. in [12].

Code multipath

The relative code multipath effects were computed as code - phase difference assuming the amplitude of phase multipath to be insignificant compared to the amplitude of the code multipath. Ionospheric effects were taken into account by the use of the relationship of two phase measurements of different frequency:

$$CMP_x = P_x - \left(\frac{2}{\alpha - 1} + 1 \right) * L_x + \left(\frac{2}{\alpha - 1} \right) * L_y \quad (1)$$

CMP_x is the estimate of the code multipath error on the pseudorange, P_x , L_x is the phase measurement of the same frequency, while L_y is the phase measurement used to correct the frequency dependent ionospheric effect. $\alpha = \frac{f_y}{f_x} = \left(\frac{f_x}{f_y} \right)^2$ describes the relationship of the ionospheric behaviour for the two frequencies.

In order to compare the code multipath level of GPS versus GIOVE-A the multipath values were sorted by a grid covering the sky with a span of 5 degree for both elevation and azimuth. Fig. 2 shows the median standard deviation of the code multipath values, derived in each grid cell per day and station, versus the elevation. No significant difference between GPS C1C and GIOVE C1B and C1C, the open code signals on G1/E1 could be found. The code multipath behaviours of the GPS precise codes are comparable with the GIOVE-A C5I, C5Q and C7Q, whereas the C8Q shows the least code multipath effects closely followed by the GIOVE-A C1A, the public regulated service (PRS).

3.2 Carrier phase analyses

Carrier phase tracking noise analyses

In the same manner as done with the code also the GIOVE-A carrier phase tracking noise can be computed as the difference of the two components (pilot - data). To accommodate for the error propagation the resulting errors were divided by $\sqrt{2}$. The resulting phase tracking noise values were sorted by elevation and can be found in Tab. 4.

In conformity with the theory, that the phase tracking noise is independent from the modulation scheme, both signals (L1B/L1C and L5I/L5Q) show the same results in the cycle domain. Looking on the results in distance domain GIOVE-A L1B/C shows up with a mean phase noise of 0.7 mm and L5I/Q with 0.9 mm. The phase noise computed within this analyses confirm previous studies [12].

Carrier phase residuals

Phase residuals contain the phase tracking noise, multipath as well as all unmodelled remaining errors like antenna cali-

bration inaccuracy and tropospheric effects. Out of that the behaviour and the magnitude of the residuals can be seen as an indicator for the observation and model accuracy as well as for measurement quality.

The following analyses base on the ionosphere free linear combination (L3: GPS L1C/L2P, GIOVE-A L1C/L7Q), computed with NAPEOS. The analyses include data of the 13 GESS over a period of 154 days.

In order to make the residuals of GPS versus GIOVE-A comparable, they were sorted into a grid with a width of one degree in both satellite azimuth and elevation. Only data of intersecting fields were compared as they might have been affected in a similar way by multipath or other disturbances.

For interpreting the data it has to be mentioned that for GALILEO 0.06 % (2501) of the ambiguities were not fixed correctly whereas for GPS all ambiguities were fixed correctly. Looking at the GIOVE-A observations correctly fixed there is a significantly larger number of rejected observations. The number of rejected observations is less by 1/3 for GPS (6 %) as for the GALILEO (9 %) data.

Fig. 3 shows the outlier cleaned mean of the residuals for GPS and GIOVE-A versus the elevation. The error bars represent the standard deviation of a single residual within a specific elevation cell. Based on the huge number of observations the uncertainty of the mean values are much smaller, in the worst case 0.06 mm for GPS and 0.2 mm for GIOVE-A. Thus for both GPS and GIOVE-A Fig. 3 shows a significant, elevation dependent effect on the residuals. Because of the appearance in both GPS and GIOVE-A and in the outlier cleaned mean over all stations this effect can not be caused by a satellite or a single station. Most probably it has to be caused by a parameter within the processing equal for all stations, as for example the antenna or any elevation dependent model or correction. This effect has to be analysed in more detail.

Due to the small number of GIOVE-A observations for elevations above 86° the outlier cleaned mean as well as the standard deviation at this elevation are not meaningful. For all elevations GIOVE-A residuals show a lower standard deviation than GPS, indicating a superior performance of GIOVE-A signals.

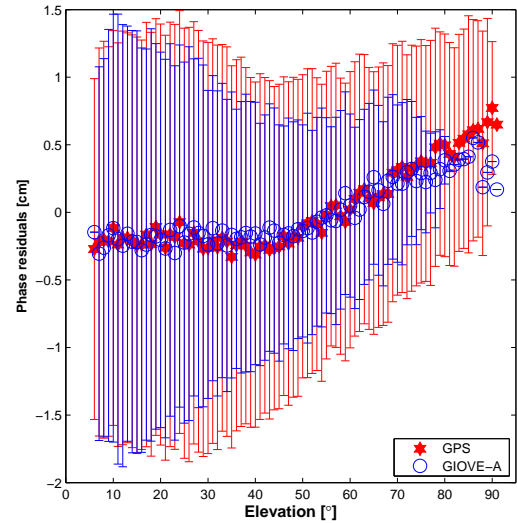


Fig. 3: Carrier phase residuals versus elevation

Elevation	C1B/C1C	C5I/C5Q
0° - 5°	0.62	0.35
5° - 10°	0.42	0.27
10° - 15°	0.33	0.21
15° - 20°	0.26	0.17
20° - 25°	0.22	0.14
25° - 30°	0.19	0.12
30° - 35°	0.16	0.10
35° - 40°	0.14	0.09
40° - 45°	0.13	0.08
45° - 50°	0.12	0.08
50° - 55°	0.11	0.08
55° - 60°	0.11	0.08
60° - 65°	0.11	0.08
65° - 70°	0.12	0.07
70° - 75°	0.12	0.07
75° - 80°	0.13	0.07
80° - 85°	0.14	0.07
85° - 90°	0.14	0.06

Tab. 3: Code tracking noise GIOVE-A [m]

Elevation	L1B/L1C		L5I/L5Q	
	cycles	mm	cycles	mm
0° - 5°	0.0095	1.81	0.0118	3.01
5° - 10°	0.0073	1.39	0.0078	1.99
10° - 15°	0.0060	1.14	0.0061	1.55
15° - 20°	0.0052	0.99	0.0054	1.38
20° - 25°	0.0044	0.84	0.0043	1.10
25° - 30°	0.0040	0.76	0.0038	0.97
30° - 35°	0.0035	0.67	0.0035	0.89
35° - 40°	0.0030	0.57	0.0031	0.79
40° - 45°	0.0027	0.51	0.0031	0.79
45° - 50°	0.0024	0.46	0.0028	0.71
50° - 55°	0.0022	0.42	0.0024	0.61
55° - 60°	0.0022	0.42	0.0023	0.59
60° - 65°	0.0023	0.44	0.0023	0.59
65° - 70°	0.0022	0.42	0.0021	0.54
70° - 75°	0.0023	0.44	0.0023	0.59
75° - 80°	0.0023	0.44	0.0023	0.59
80° - 85°	0.0024	0.46	0.0022	0.56
85° - 90°	0.0024	0.46	0.0022	0.56

Tab. 4: Carrier phase tracking noise GIOVE-A

L1C/C1C - L7Q/C7Q							L1A/C1A - L7Q/C7Q						
obs	rej	rej[%]	mean	rms	mean	rms	obs	rej	rej[%]	mean	rms	mean	rms
811	102	12	0.384	14.287	-160	1368	748	156	20	0.467	13.937	-187	874
867	157	18	-0.384	18.646	-201	1275	653	267	40	-1.347	18.607	-144	785
732	162	22	-1.047	17.936	-157	1222	519	246	47	-1.082	15.104	-209	784
665	98	14	-0.789	13.766	-165	1375	661	112	16	-0.480	12.625	-176	958
765	201	26	0.301	18.307	-198	1241	648	316	48	-0.922	15.706	-227	978
735	107	14	-0.337	15.665	-181	1308	693	131	18	-0.718	15.484	-186	797
788	74	9	-0.280	17.553	-24	1334	790	73	9	-0.079	17.251	-88	894
791	152	19	-0.590	16.122	-136	1257	794	158	19	-0.058	15.830	-122	817
805	150	18	-0.604	15.956	-211	1285	712	145	20	-1.044	13.706	-264	907
723	192	26	1.357	19.612	-171	1330	590	198	33	1.662	15.361	-235	971
661	146	22	-0.301	17.757	-211	1365	686	113	16	-0.406	18.046	-182	962

Tab. 5: Phase/Code validation [mm]

3.3 Phase and code validation in processing

Looking on the code and phase quality of the different signals, it was conspicuous that GIOVE-A C1A/L1A and C8Q/L8Q ranks best, whereas for the current processing of GIOVE-A data usually the C1C and C7Q signals are used. This leads to the question of the best signal combination for GIOVE-A. Hence we processed 10 days of GIOVE-A data, using different signal combinations. Presently the processing of the C8Q/L8Q signals is not yet implemented NAPEOS. However, the GIOVE-A C1A/L1A - C7Q/L7Q combination succeeded, as seen in Tab. 5. The RMS of the code results can be reduced by approximately a factor of 1.4, whereas the RMS of the phase observations shows only a minor improvement. Furthermore it causes a higher number of rejected observations. As for the case of the C1A/L1A - C8Q/L8Q combination, for the L1A/C1A - C7Q/L7Q combination as well, further analyses have to be carried out to evaluate potential benefits of these combinations.

3.4 Conclusion data quality

- The analyses of GIOVE-A E1 and E5 code/carrier phase noise confirmed the good results from prior analyses.
- The GPS C1C and the GIOVE C1B and C1C show a comparable multipath behaviour.
- The multipath of the GPS precise codes C1P and C2P show is comparable to the GIOVE-A C5I, C5Q and C7Q
- The GIOVE-A C8Q shows the least code multipath behaviour closely followed by the C1A
- The combination C1A/L1A - C8Q/L8Q should show the best noise behaviour, whereas NAPEOS cannot process this combination. Further tests have to show the reasons for this.
- The carrier phase residuals show a small elevation dependent bias. Further analyses have to show the reasons.

4 Orbit Quality

In this section we will assess the quality of our precise orbit determination solutions. We have 3 sets of different orbit solutions. The first set are the 7-day solutions based solely on SLR observations. Set 2 being the solutions based on the microwave observations using 1- to 5-day arcs. Set 3 being the solutions based on a joined analysis of the microwave and SLR observations also using 1- to 5-day arcs.

First we will make an assessment of the orbit quality by looking at the internal consistency of the solutions. For the two sets using microwave observations the internal orbit consistency is done using an orbit fit. This will not tell us much about the absolute quality of the solutions but it will indicate the optimal arc length and whether adding the SLR observations to the microwave data improves the orbit estimates.

Secondly we will validate the orbits by determining the SLR residuals. Of course the solutions which used SLR observations should perform better than the microwave only solutions. However, the validation of the microwave orbits against the SLR observations will give us a good impression of the absolute accuracy of our orbits.

	Microwave only					Microwave and SLR				
	1d	2d	3d	4d	5d	1d	2d	3d	4d	5d
Part 1	662	254	146	131	127	505	172	110	81	84
Part 2	221	99	52	41	42	185	80	41	34	31
Total	395	162	90	78	76	316	117	69	53	52

Tab. 6: Internal Orbit Consistency [mm]

As a third test we will compare the best orbit (best arc-length) of each of the three sets (set 1 only has one arc-length) against each other. This should give us an other indication of the quality of the orbits.

Last but not least we will have a look at the solar radiation pressure parameters that were estimated.

4.1 Internal Orbit Consistency

To determine the internal orbit consistency of the different solutions we will make an orbit fit. For this orbit fit test we will use the middle 24 hours of two consecutive solutions and fit one 48-hour arc through these two parts. For this fit the satellite orbit is modelled by estimating the satellite state vector and all nine parameters of the extended CODE orbit model. The RMS of this fit gives us a indication of the internal consistency of the orbit estimates. For longer-arcs the RMS of fit should go down because the solutions are not fully independent from each other. So a lower RMS for the longer arc solutions is to be expected. However, on the other hand this means that if the RMS does not go down with increasing arc length that we have reached the limit of our modelling capabilities. Furthermore, comparing the internal orbit consistencies of equal length solutions will tell us which solution has a better internal consistency. The results of this internal orbit consistency check are given in Tab. 6. The table gives the mean of the 2-day RMS over all processed days. The mean is given separately for the first and second part of the observation interval and also for the total observation interval.

There are several interesting results visible in Tab. 6. First of all it shows that the results of part 2 of the observation interval are significantly better than the results from part 1. The reason for this is unclear since the statistics from the 1-day solutions, e.g. residual rms, number of observations, and such did not significantly change after the observation gap. The improvement, however, is very significant. The second observation is that the results including the SLR observations are significantly better compared to not including the SLR observations. This is true for all arc lengths! As expected we see a significant improvement of the internal consistency when going from 1-day arcs to 3-day arcs. The 4-day arcs show only a slight improvement compared to the 3-day arcs. The 5-day arcs do not show a significant improvement. This indicates that with the current observations and modelling techniques the optimal arc-length for precise orbit determination seems to be around 3- to 4-days.

4.2 SLR Validation

In this section we look at the SLR residuals obtained from the different orbit solutions. A clean SLR dataset was generated by using the SLR only orbit to remove any outliers in the SLR observations. The total number of valid SLR normal points for the entire period is 3520 observations from 17 different SLR stations. The number of observations for the Part 1 is 796 points from 12 stations and for Part 2 is 2724 normal points from 17 stations. For two of the three solutions the SLR data has been used in the orbit determination process so the residuals will give a too optimistic indication of the orbit quality.

As can be seen from the table the 3-day solution based on the microwave data only has the lowest SLR residuals and indicate a radial precision of around 100 mm. A similar behaviour can be seen in the microwave plus SLR solution with the exception of the 1-day solution (and to a smaller extend also the 2-day solution) were the orbit solution is mainly driven by the SLR data but the quality as can be seen from the internal consistency of the orbit is poor. Interesting to notice is the large improvement in SLR residuals for the microwave plus SLR solution although the number of SLR data points is only 2 % of the total tracking data in the combined solution. The values for the SLR only solution are included to give an indication of the lowest possible SLR residuals one could expect by combining the microwave and SLR data.

	SLR only	Microwave only					Microwave and SLR				
	7d	1d	2d	3d	4d	5d	1d	2d	3d	4d	5d
Part 1	54	1046	448	280	316	333	91	120	124	168	167
Part 2	76	375	228	200	214	214	98	121	136	160	168
Total	72	597	293	221	241	246	96	120	133	162	167

Tab. 7: Two way SLR residuals [mm]

Solution	Radial	Trans.	Cross	3D-RMS	Typical RMS
micro vs. SLR	93	510	396	652	377
micro+SLR vs. SLR	73	450	369	587	339
micro+SLR vs. micro	46	169	137	222	128

Tab. 8: Orbit Comparison in [mm]

4.3 Orbit Comparison

To get an indication of the overall orbit quality the best solutions are compared against each other for the period covered by Part 2. The table above gives the RMS differences between the SLR only (SLR), 3-day microwave only (micro) and the 3-day microwave and SLR solution (micro+SLR).

As expected the largest difference is between the SLR only and microwave only solution giving a total orbit difference of 652 mm. As a major part of the SLR tracking from GIOVE-A comes from European stations the quality of the SLR solutions is directly correlated with the ability of the European stations to track GIOVE-A i.e., bad weather over Europe can lead to data gaps for more than 24 hours impacting the orbit quality. Interesting is to see the large impact the SLR data has on the combined solution. As mentioned before the SLR data is only around 2 % of the total tracking data but has a significant impact on the orbit solution as can be seen from the difference between the microwave only and microwave plus SLR solution.

4.4 GIOVE-A Solar radiation pressure

Based on the analysis presented above we conclude that the 3-day solution using both microwave and SLR observations has given the best orbit estimates. Now we will use this solution to have a look at the time series of the estimated solar radiation pressure parameters. As for all GNSS satellites the major disturbing force acting on the GIOVE-A satellite is the solar radiation pressure. In our analysis we have used no a priori model to account for these affects but have estimated 5 parameters from the extended CODE orbit model. The extended CODE orbit model consists of 9 parameters, 1 constant and two periodic terms in a 3-axis system (D, Y, and B) defined by the sun-satellite geometry. The D-axis is in the sun-satellite direction. The Y-axis is perpendicular to the sun-satellite and satellite-earth direction, and typically is the axis around which the solar panels are rotated. The B-axis complements the right handed 3-axis system. From the 9 possible parameters we have estimated 5, the constant terms in all three directions and the periodic terms in the B-direction.

Fig. 4 shows the evolution of the main solar radiation pressure term D0, the constant term estimated in the satellite-sun direction. There are two interesting aspects in this figure. First of all the mean value of the D0 term ($-97 * 10^{-9} m/s^2$) which is, as expected, very close to the typical values obtained for the other GNSS systems GPS and GLONASS. The second aspect is the very noisy behaviour of the estimates in the first part of the results especially when compared to the relatively smooth part for the second part of the results. These results must be correlated with the significant improvement we observed in our internal orbit consistency checks when comparing the two observation parts with each other. One can easily imagine that if the repeatability of the estimated solar radiation pressure parameters improves it will be easier to model the orbit of the satellite especially over longer arcs. The open question is why the behaviour of the solar radiation pressure parameters changes so drastically. Was a real change (e.g. satellite or solar panel attitude control) made during the satellite maintenance in February 2007 or is it caused by the satellite orbit geometry?

Looking at the other estimated solar radiation pressure parameters we notice that the constant and the cosine term in the B-direction show a similar behaviour as the D0 term, noisy in part 1 of the data smooth in part 2. The constant term in the Y-direction and the sine term in the B-direction are equally well determined in both parts of our data set.

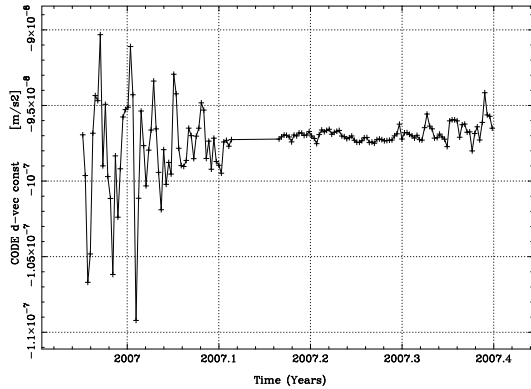


Fig. 4: The evolution of the constant solar radiation pressure term (DO)

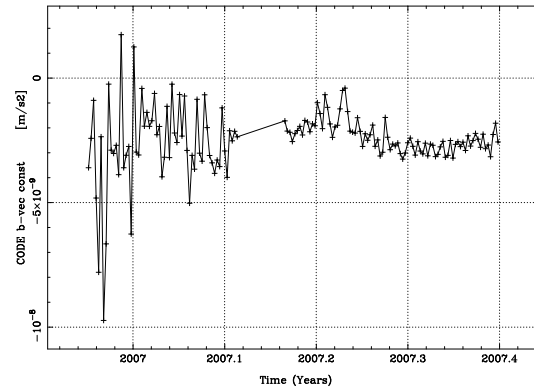


Fig. 5: The evolution of the constant solar radiation pressure term in the B-direction (BO)

The last interesting aspect we noticed in the solar radiation pressure parameters is that the constant term in the B-direction (B0) has a significant non-zero value. Fig. 4 shows the time series of the B0 estimates.

When using only the last (smooth) part of the estimates the value of B0 is $-2.3 \times 10^{-9} m/s^2$ whereas the sigma of the B0 values around this mean value is only $0.6 \times 10^{-9} m/s^2$. For GPS satellites the size of the B0 term is much smaller $0.4 \times 10^{-9} m/s^2$ [13]. This indicates that a significant force is working in this B-direction. A possible cause could be a misalignment of the solar panel axis (rotation of the solar panel around the Y-axis), i.e., solar panel axis not perpendicular to the sun-satellite direction. Based on the observed size of the effect the misalignment would have to be of the order of 1.4 degrees, which is not impossible. The constant term in the Y-direction, in GPS often referred to as the Y-bias, is very small ($0.1 \times 10^{-9} m/s^2$) and actually much smaller than the Y-bias observed for the GPS satellites ($\sim 1.0 \times 10^{-9} m/s^2$). This indicates that sun pointing of the satellite, rotation around the satellite body fixed Z-axis, is very accurate. Nevertheless, we are convinced that also for GIOVE-A a Y-bias must be taken into account, especially during the eclipse season where we can see some significant effects in the Y-bias.

If we look at estimates of the periodic terms in the B-direction we notice that the sigma of the estimates around the mean is at the same order or even larger than the mean itself. This indicates that these terms are not really significant. To test whether the estimation of these periodic terms is really needed we generated 2-, 3-, 4-, and 5-day solutions using the combined microwave and SLR observations and estimating only the three constant solar radiation pressure terms and used our internal orbit consistency check to validate the obtained orbits. The results of the orbit fit are given in Tab. 9, column DOY0B0.

For all four solutions the RMS of the orbit fit went up significantly. If we look at the 3-day solutions the orbit fit RMS went from 110 mm to 408 mm, and from 41 mm to 101 mm for part 1 and part 2 of the data respectively. Similar changes are observed for the other arc-lengths. So first of all this demonstrates that the estimation of these periodic terms is really needed to get precise orbit estimates, despite the fact that the estimated values are not very repeatable. Secondly for part 1 of the analysed data the RMS increases with a factor of 4 whereas for the second part the increase is a factor of 2.5. This once again underlines that there are some significant unmodelled perturbations acting on the satellite in the first part of the data period.

In the past it has been shown that for GPS satellites the estimation of periodic terms in both the D- and the B-direction gives superior results compared to estimating them only in the B-direction [14]. The main problem with this combination is that these parameters correlate very strongly with the estimation of the length of day (LOD) and therefore it is not commonly used in the IGS analysis of the GPS data. In our current investigation we are not very interested in LOD so we decided to test the estimation of the periodic parameters in the D-direction. To test the significance of the constant term in the B-direction we made two different solutions, again using the combined microwave and SLR observations. One solution estimating the three constant terms and the periodic terms in the D- and B-directions (DOY0B0DpBp). The second

	D0Y0B0				D0Y0B0DpBp				D0Y0DpBp			
	2d	3d	4d	5d	2d	3d	4d	5d	2d	3d	4d	5d
Part 1	474	408	426	411	206	117	86	88	231	162	134	132
Part 2	135	101	110	106	90	44	35	33	103	54	46	42
Total	273	227	239	230	137	74	58	55	155	98	82	78

Tab. 9: Internal Orbit Consistency [mm]

solution was identical to the first except for the estimation of the constant parameter in the B-direction (D0Y0DpBp). Again we made solutions with arc-lengths from 2- to 5-days. The results of these tests are also included in Tab. 9. The differences between these two solutions demonstrate that, as expected, the B0 term is quite significant, all orbit fit rms values are significantly higher for the solution where B0 was not estimated. Furthermore, when comparing these results with those given in Tab. 6 we do not see any improvement when estimating the periodic terms in the D-direction.

5 Conclusion

The analyses of the observation data quality (signal quality) confirmed the good results from prior analyses for code multipath behaviour and code noise. GPS C1C and the GIOVE-A C1B/C1C show a comparable multipath behaviour, whereas the GPS precise codes C1P/C2P are comparable to the GIOVE-A C5I, C5Q and C7Q. The least code multipath behaviour could be found for GIOVE-A C8Q, closely followed by the GIOVE-A C1A. Based on this, the combination C1A/L1A - C8Q/L8Q should show the best noise behaviour within the processing. Unfortunately it cannot be processed using the current software. Further tests have to show the reasons for this.

The results in this paper demonstrate that the 13 station GESS network allow us to determine the orbit of the GIOVE-A satellite quite accurately (200 mm) using only microwave observations. The SLR validation of the microwave orbits gives an RMS of 100 mm (one way range RMS). This gives an absolute value for the orbital error. Of course the SLR observations mainly tell us something about the radial orbit errors, the along- and cross-track errors could be much higher. To obtain accurate GIOVE-A orbit estimates the orbits and clock of the GPS satellites, tracked simultaneously with the GIOVE-A satellite, have to be kept fixed using the IGS final orbit and clock products [4]. Furthermore, an arc-length of 3-days should be used. An arc length of 2-days also produces good results but the 3-day results seem to be better. An arc length of 4-days produces good results as well but arcs longer than 4-days seem to suffer from orbit modelling problems. The microwave based orbit estimates may be improved by adding the available satellite laser ranging (SLR) observation in the orbit estimation process. Although there are very few SLR observations they do have a very significant positive effect on the orbit estimates improving the internal consistency from 52 mm to 41 mm. Also the validation of the orbits using the SLR observations shows a significant improvement. However, this is not an independent validation because the same SLR observations were used in the orbit determination.

In orbit arcs longer than 3-days the orbit determination seems to start to suffer from modelling problems. With the current orbit determination accuracy of ~ 200 mm this is somewhat surprising. A closer look at the solar radiation pressure term showed two interesting features. First a dramatic change of the repeatability of the estimated solar radiation pressure parameters. Secondly, a significant non-zero value for the constant solar radiation pressure parameter in the direction of the B-axis. Both these effects indicate that the GIOVE-A solar panel or attitude alignment are not 100% correct. It is not clear why the behaviour of the estimated solar radiation parameters has changed so significantly. However, the effect on the intern orbit consistency check is very remarkable indicating that for the first part of the data some significant unmodelled forces are acting on the satellite.

GIOVE-A is a test satellite not necessarily ready for scientific use. However the orbit analysis, with an accuracy presently not sufficient for scientific use, can help to identify weaknesses and room for improvements. The accuracies routinely achieved for the GPS satellites within the IGS are an order of magnitude better. The question is whether this is caused by the limited ground station tracking network (only 13 sites) or by the in orbit behaviour of the GIOVE-A satellite itself or a combination of both factors. To answer this question we treated a GPS satellite exactly the same way as the GIOVE-A satellite, i.e., also estimating a intersystem bias for the GPS satellite using only the 13 GESS stations. So the treatment of the GPS satellite and the GIOVE satellite was identical. The direct comparison showed, that the GIOVE-A orbits are less accurate than the GPS orbits. This speaks against a limiting influence of the GESS network configuration.

It has to be noticed that for GIOVE-A still many things are need to be improved. The results presented within this paper

can be used as first attempt towards an optimal processing approach with GALILEO in future.

6 Future work

For the near future it is planned to analyse the different signal combinations in order to find the best possible combination for the processing.

Furthermore, we will expand the analysis time period to verify whether the behaviour of the solar radiation pressure parameters remains smooth. If it remains smooth that would indicate that the satellite behaviour has changed somehow during the maintenance in February 2007. If the parameters become "noisy" again it means that it is caused by the orbit geometry.

Last but not least, we will make a more enhanced analysis of the solar radiation pressure parameters by analysing the data using different combinations of the 9 available solar radiation pressure parameters.

References

- [1] G. Beutler, J. Kouba, and T. A. Springer. "Combining the Orbits of the IGS Processing Centers". *Bulletin Géodésique*, 69(4):200–222, 1995.
- [2] M. Crisci, M. Hollreiser, M. Falcone, M. Spelat, Giraud J., and S. La Barbera. "GIOVE mission sensor station receiver performance characterization: preliminary results". In *NAVITEC, December 2006*, December 2006.
- [3] US DoD. "Global positioning system standard positioning service performance standard.". Technical report, U.S. Department of Defense, October 2001 2001.
- [4] J. M. Dow, R. E. Neilan, and G. Gendt. "the International GPS Service: Celebrating the 10th anniversary and looking to the next decade". *Advances in Space Research*, 36:320–326, 2005.
- [5] EU-Commission. "GALILEO mission high level definition". Technical report, European Commission and ESA, 23. September 2002 2002.
- [6] W. Gurtner and L. Estey. "*RINEX The Receiver Independent Exchange Format Version 3.00*", June 14 2007.
- [7] Y. Hatanaka. "IGS electronic mail 06 jun 01:25:56 PDT 2007 message number 5609". Available at <http://igs.cb.jpl.nasa.gov/mail/igsmail/2007/msg00089.html>, June 2007.
- [8] M. Irsigler and B. Eissfeller. "Comparison of multipath mitigation techniques with consideration of future signal structures". In *Proceedings of the 16th International Technical Meeting of the Satellite Division of the Institute of Navigation, ION GPS/GNSS 2003, September 9-12, 2003, Portland, Oregon, 9.-12. Sept 2003*.
- [9] A. E. Niell. Global Mapping Functions for the Atmosphere Delay at Radio Wavelengths. *Journal of Geophysical Research*, 101(B2):3227–3246, 1996.
- [10] T. Pany, M. Irsigler, B. Eissfeller, and J. Winkel. "Code and carrier phase tracking performance of a future galileo rtk". In *Proceedings of the European Navigation Conference ENC-GNSS 2002, Copenhagen, Denmark, 27-30 May 2002, 2002*.
- [11] J. Saastamoinen. "Contributions to the theory of atmospheric refraction. part ii. refraction corrections in satellite geodesy.". *Bull. Géod., Nouvelle Sér., Année 1973, No. 107, p. 13 - 34*, 107:13–34, 1973.
- [12] A. Simsky, J.-M. Sleewaegen, M. Hollreiser, and M. Crisci. "Performance assessment of galileo ranging signals transmitted by gsb-v2 satellites". In *ION GNSS, September 2006*, 2006.
- [13] T. A. Springer, G. Beutler, and M. Rothacher. "A new solar radiation pressure model for GPS satellites". *GPS Solutions*, 2(3):50–62, January 1999.
- [14] T.A. Springer, G. Beutler, and M. Rothacher. "Improving the Orbit Estimates of the GPS Satellites". *Journal of Geodesy*, 73(3):147–157, 1999.